NAVIER-STOKED

Spring 2023 ME Executive Summary

Design Team

Thomas Chan, Maya Kesapradist, Connor Lam, Jonathan Neves, Ash Wu, Perry Yee

Design Advisor

Prof. Marguerite Matherne

Abstract

The Navier-Stokes equations are a vital part of fluid mechanics describing the flow of viscous fluids. Working with these equations can be difficult and understanding the theory behind the equations is even more of a challenge for students. In an undergraduate course, an important aspect of solving problems with these equations are the conditions and assumptions that allow the equations to be simplified. Students tend to have trouble understanding when the assumptions apply as well as the effect of these assumptions on the equations. This incomplete comprehension of the concept results in poor test scores. The goal of the project was to boost student learning outcomes by visualizing Navier-Stokes using a physical model of flow between two parallel flat plates. The rig is composed of several key components: steady-the main acrylic tank, an aluminum support frame, a camera with a laser for particle visualization, and a piping system for fluid movement. As fluid cycles through our system, output velocity collected by particle image velocimetry and pressure measurements collected by pressure transducers indicate the validity of assumptions such as the steady state condition, the infinite plates condition, and the fully developed condition. These assumptions are powerful as they allow students to eliminate many terms in the Navier-Stokes equations, allowing them to be solved analytically. While the design of the rig is complete, user testing will be conducted in a few months to quantify the impact of our solution. We anticipate our project will lead to increased student comprehension of these assumptions shown through improved student scores.

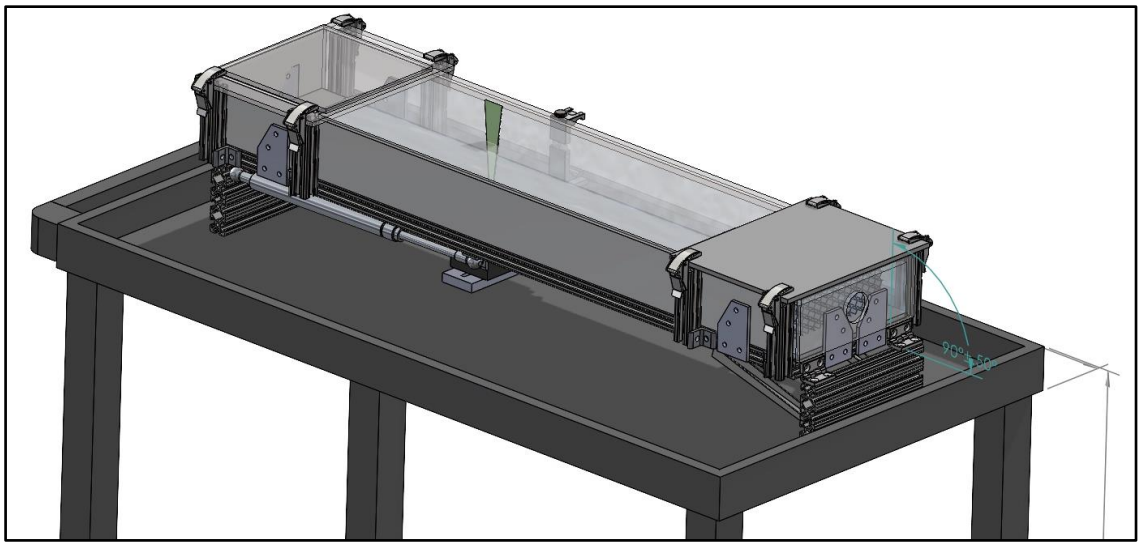

For more information, please contact m.matherne@northeastern.edu

Need

Fluid mechanics is a critical course for every mechanical engineering student. An important component of this course is the Navier-Stokes equations which describes the motion of viscous fluids. Students tend to find the overall course confusing; however, the Navier-Stokes portion is especially challenging. Professors found that students particularly have trouble identifying the assumptions needed to simplify and solve the equations. There are a handful of vital assumptions (such as the steady state condition) that result in simplification that can eventually lead to analytical solutions. If students are unable to apply the assumptions, then they cannot even begin to solve questions leading to low scores and even lower motivation. Our client and advisor, Professor Matherne, realized this problem and thought a teaching aid would be useful. Our team was tasked with creating a teaching aid that could mimic various situations and highlight relevant assumptions specifically for scenarios where flow is between flat plates.

Background and Significant Prior Work

The Navier-Stokes equations, the core of our project, are presented below with equations 1-4.

$$\frac{\partial u}{\partial x}+\frac{\partial v}{\partial y}+\frac{\partial w}{\partial z}=0 \tag{1}$$

Equation 1 is the general form of the continuity equation for incompressible flow in three dimensions where u, v, w are the velocities in the x, y, and z-directions respectively and, $\frac{\partial}{\partial x}, \frac{\partial}{\partial y}, \frac{\partial}{\partial z}$ are the partial derivatives of the x, y, and z-directions respectively. The continuity equation fulfills the conservation of mass requirement, but conservation of momentum still needs to be met. Since velocity is frequently computed in a 3D vector space, it often makes sense to create a momentum equation for each direction as seen with equations 2-4 below:

$$x: \rho\left(\frac{\partial u}{\partial t}+u\frac{\partial u}{\partial x}+v\frac{\partial u}{\partial y}+w\frac{\partial u}{\partial z}\right)=-\frac{\partial p}{\partial x}+\rho g_x+\mu\left(\frac{\partial^2 u}{\partial x^2}+\frac{\partial^2 u}{\partial y^2}+\frac{\partial^2 u}{\partial z^2}\right) \tag{2}$$

$$y: \rho\left(\frac{\partial v}{\partial t}+u\frac{\partial v}{\partial x}+v\frac{\partial v}{\partial y}+w\frac{\partial v}{\partial z}\right)=-\frac{\partial p}{\partial y}+\rho g_y+\mu\left(\frac{\partial^2 v}{\partial x^2}+\frac{\partial^2 v}{\partial y^2}+\frac{\partial^2 v}{\partial z^2}\right) \tag{3}$$

$$z: \rho\left(\frac{\partial w}{\partial t}+u\frac{\partial w}{\partial x}+v\frac{\partial w}{\partial y}+w\frac{\partial w}{\partial z}\right)=-\frac{\partial p}{\partial z}+\rho g_z+\mu\left(\frac{\partial^2 w}{\partial x^2}+\frac{\partial^2 w}{\partial y^2}+\frac{\partial^2 w}{\partial z^2}\right) \tag{4}$$

where u is the velocity in the x-direction, v is the velocity in the y-direction, w is the velocity in the z-direction, ρ is the density of the fluid, $\frac{\partial}{\partial t}$ is the partial derivative with respect to time, $\frac{\partial}{\partial x}, \frac{\partial}{\partial y}, \frac{\partial}{\partial z}$ are the partial derivatives of the x, y, and z-directions respectively, $\frac{\partial p}{\partial x}, \frac{\partial p}{\partial y}, \frac{\partial p}{\partial z}$ are the partial derivatives of pressure with respect to the x, y, and z-directions respectively, g_x, g_y, g_z are the components of gravity in the x, y, and z-directions respectively, μ is the viscosity of the fluid, and $\frac{\partial^2}{\partial x^2}, \frac{\partial^2}{\partial y^2}, \frac{\partial^2}{\partial z^2}$ are the second partial derivatives with respect to the x, y, and z-directions respectively.

As you can see from equations 1-4 above, the Navier-Stokes equations are quite detailed and complex. The complexity increases for students when they have to determine the assumptions and simplifications to make such as the steady state condition ($\frac{\partial}{\partial t} = 0$), the infinite plates condition ($v, w = 0$), the plane flow assumption ($\frac{\partial}{\partial z} = 0$), and the fully developed condition ($\frac{\partial u}{\partial x} = 0$). Students often look for keywords for applying the appropriate assumptions, but it is important for them to actually understand the theory when applying the Navier-Stokes equations.

The steady state condition leads to the simplification $\frac{\partial}{\partial t} = 0$ in which there is no variable change with respect to time. If you have infinite plates without fluid and insert fluid into the system, it will take time for the fluid to develop. The fluid interacts with the plates, the plates interact with the fluid, and the particles within the fluid interact with each other. The system eventually reaches an "equilibrium" where variables like velocity no longer change with additional time. The infinite plates condition leads to the simplification $v, w = 0$. If you have fluid within a duct, the walls of the tube influence the fluid profile. If you move the walls away from the flow, the wall effects are shifted away. If you take this to the extreme and move the walls infinitely away, the effects are shifted infinitely away [1]. The fluid has no desire to move in the y and z directions leading to $v, w = 0$. The plane flow assumption leads to the simplification $\frac{\partial}{\partial z} = 0$. Due to the interaction between the fluid and plates in this scenario, there is no variable change with regard to the z-direction. The fully developed condition leads to the simplification $\frac{\partial u}{\partial x} = 0$. This is slightly different from the steady state condition. The steady state condition means variables are not changing with time whereas fully developed means the variables are not changing with position (x direction). A system can be in a steady state, but not fully developed.

A physical model of fluid flow highlighting the effects of these assumptions would help students develop an intuitive understanding of how to simplify the Navier-Stokes equations. Research suggests that physical models boost learning in science-based concepts for both struggling and excelling students. For instance, Newman et al. [2] show that students (regardless of prior performance) in an undergraduate biology class tended to score higher on assessment questions that were supported by activities involving physical models. After a learning session, students answered correctly on questions supported by model-based activity 25% more frequently compared to just 13% on questions without model support. Physical models also do not interfere with other teaching aids: Dori and Barak [3] show that physical models have a positive effect on learning outcomes when combined with other teaching strategies such as the use of virtual models in organic chemistry. While fluid mechanics is different from biology and chemistry, they are similar in how visualization is key to understanding. While fluid visualization systems have been built for use in research labs, one tailored for use as a teaching aid does not exist yet.

The existing technologies used to visualize flow in research labs include ink in pipe, Schlieren photography, and particle image velocimetry (PIV). Ink in pipe [4] is a solely visual method where ink is injected into round tubing. While this provides a clear visual of the velocity profile, the visuals would degrade as the fluid darkens and no quantifiable data could be collected. On the other hand, Schlieren photography is a visualization technique that takes advantage of the fact that light distorts differently depending on the density of the material it passes through with a camera capturing the changes [5]. This method requires an intricate setup and only works with density differences; however, the Navier-Stokes equation describes incompressible fluids, meaning density is constant. Finally, particle image velocimetry (PIV) is a fluid visualization method characterized by tracking particles placed in moving fluid [6]. The PIV method provides a visual model for students to see differences in fluid velocities, and provides measurable values for students to use in fluid flow calculations. Students use the velocities found in the PIV system to confirm the relationship between pressure and velocity, to confirm the assumption of infinite plates, and to

understand the velocity gradient in a visual platform. The relative ease of PIV setup also meant this visualization technique was well suited to be adapted for a classroom environment.

Design Solution

Our team was asked to "design a physical model of [laminar] flow between flat plates that can be manipulated and report the fluid velocity at various points." The model would be used as a portable teaching device. To fulfill this need, a long rectangular tank was built to approximate flow between flat plates. Pipes connected to the two ends of the tank circulate fluid through a pump, while particles in the fluid are tracked to report the fluid velocity. The angle of the tank can be manipulated to simulate different flow conditions as shown in Figure 1 below.

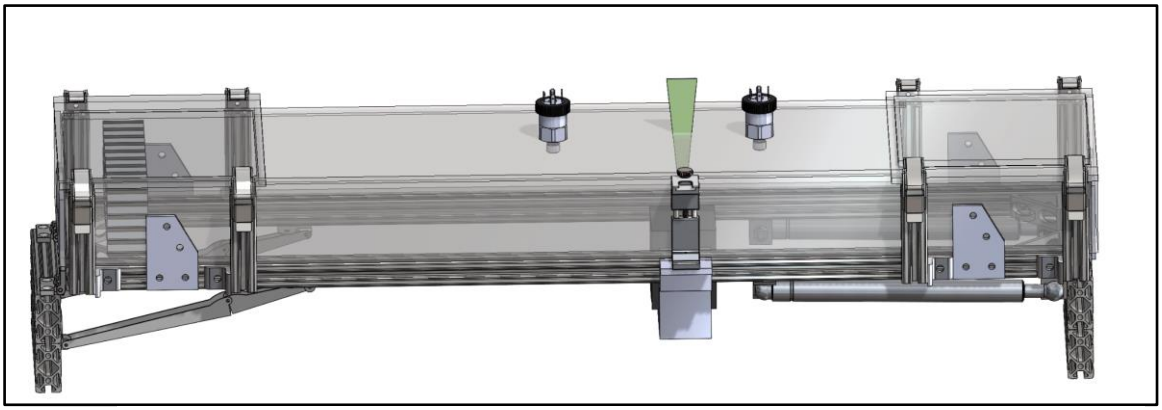

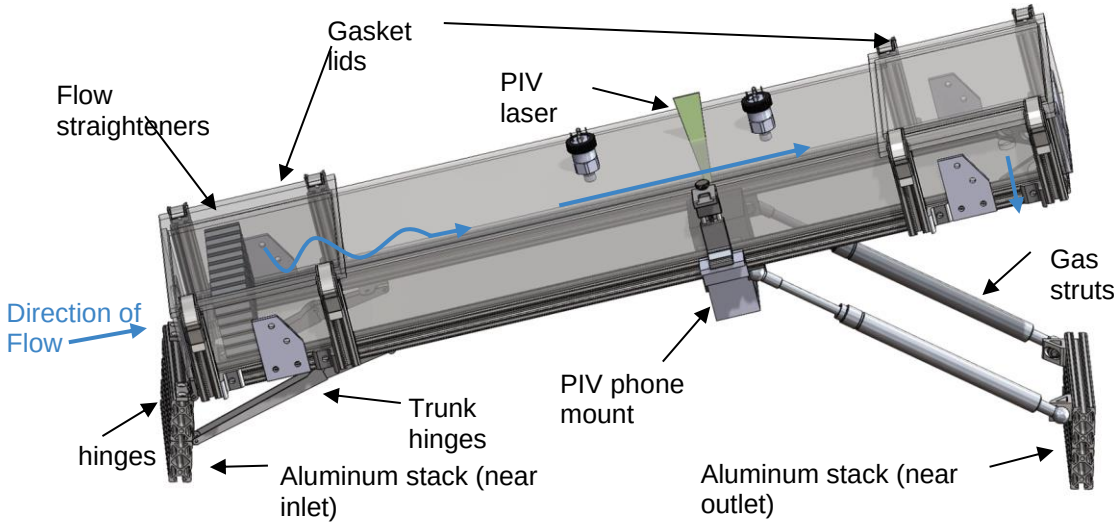

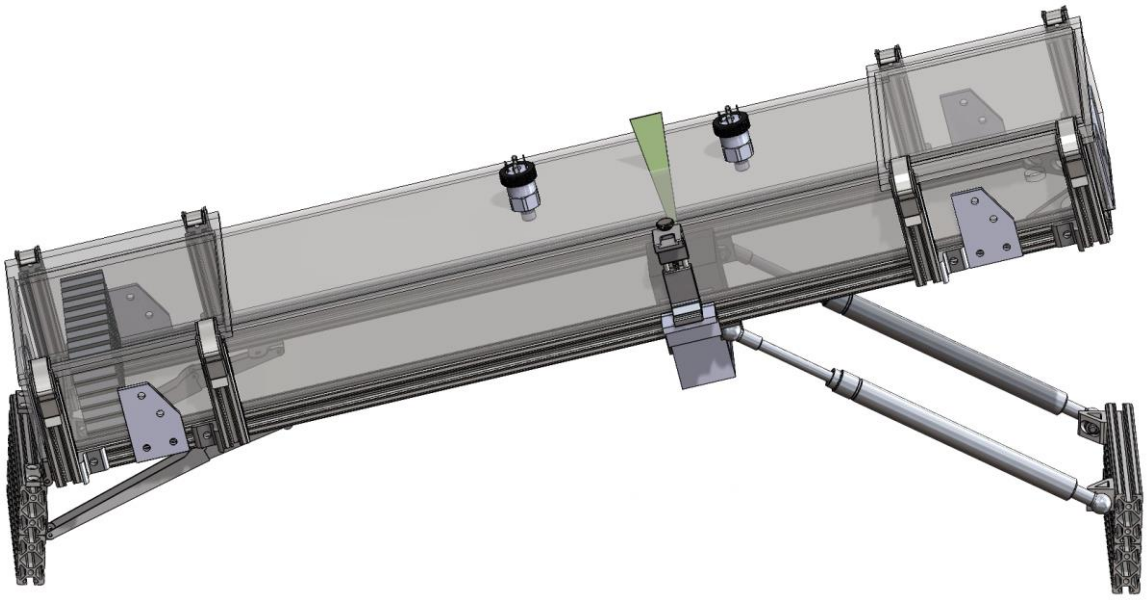

Figure 1: The tank can be configured in two positions: with no angle or a 30 degree angle.

The centerpiece of our design is the 3” x 8” x 40” tank constructed of 0.25” thick acrylic. The tank is supported by 1” x 1” aluminum extrusions mounted to a wheeled cart. The dimensions of the tank were chosen in order to ensure portability and laminar flow. The tank is more portable at a smaller size, but it is more difficult to achieve laminar flow at small sizes. The 3” by 8” cross section meant the flow would have a Reynolds number of 45 – well within the laminar regime – with an entrance length of no more than 12”. The total length of the tank was set to 40” in order to ensure there is sufficient length to observe fully developed laminar flow. Two lids on top of the tank serve two purposes: to speed up the process of filling the tank and to provide access for cleaning and maintenance. Gaskets on the bottom of these lids and latches on the top prevent fluid leakage and ensure the tank remains a closed system.

The frame of the tank is supported by two aluminum stacks. Rotational hinges attached to the inlet stack enable the user to manipulate the angle of the tank. When the system is rotated, a set of trunk hinges lock the system at 30 degrees. Gas struts help lift the system as the angle is adjusted to minimize the weight of the fluid.

The fluid within the tank is composed of a 70% glycerin 30% water mixture. The glycerin content increases the viscosity of the fluid, which reduces the Reynolds number to maintain laminar flow. To circulate fluid through the tank, pipes are attached to the two ends of the tank. The fluid and piping components are described in the P&ID (piping and instrumentation diagram) as shown in Figure 2 below.

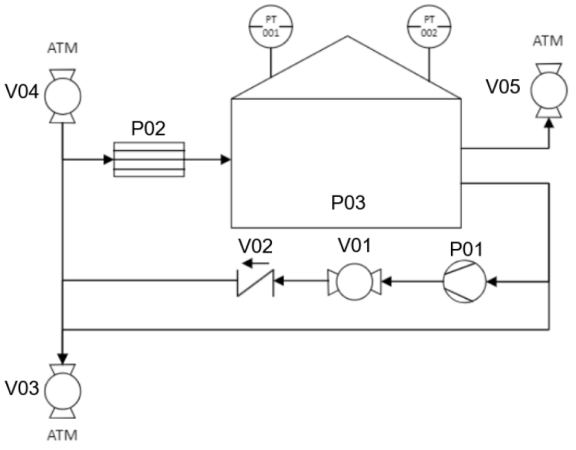

Element ID	Description	Element ID	Description
V01	Flow Ball Valve	P01	Gear Pump
V02	Flow Check Valve	P02	Flow Straightener
V03	Drain Ball Valve	P03	Flow Tank
V04	Fill Ball Valve	PT001	Inlet Pressure Transducer
V05	Drip Ball Valve	PT002	Outlet Pressure Transducer

Figure 2: Piping and instrumentation diagram of tank fluid system

Flexible PVC tubing connects the main tank to a pump that circulates the fluid. The adjustable 24VDC pump can transfer a maximum of 1250 GPH and generate up to 13.1 feet of head. In other words, the maximum pump delivery pressure is 6.769 psi for the glycerin-water mixture. The required delivery pressure needed to produce our ideal laminar flow at a Reynolds number of 45 was about 1.124 psi, which would result in an average fluid velocity of about 0.47 in/s in the tank. A slow speed was necessary in order to minimize the Reynolds number and ensure laminar flow.

Additional piping components spliced throughout the tubing and our system allow the user to observe, manage, and maintain the fluid. The first component is a fill valve (V04) that allows the user to connect to an external hose or funnel to fill the tank. The system will be fully filled and primed with no remaining air when fluid is seen exiting through the drip valve positioned at the highest point in the system (V05). When the fluid is transported from the pump to the entrance pipe, the fluid exits as a concentrated, high velocity jet. A flow straightener breaks up this jet of fluid to ensure laminar flow as detailed in the Appendix. Once the fluid is past the straightener, two pressure transducers in the main tank report pressure to highlight one of the Navier-Stokes solving assumptions.

The fluid exits the tank through flexible PVC piping and enters our pump, which pushes the fluid forward through the flow valve (V01). This valve will be open for all cases where flow is needed, but can be closed to stop the system for any reason. The final component the fluid will pass before entering the tank is the drain valve (V03). This valve will allow the user to drain the tank for cleaning and maintenance purposes. The last main feature of our design is the particle image velocimetry as pictured in Figure 3 on the following page.

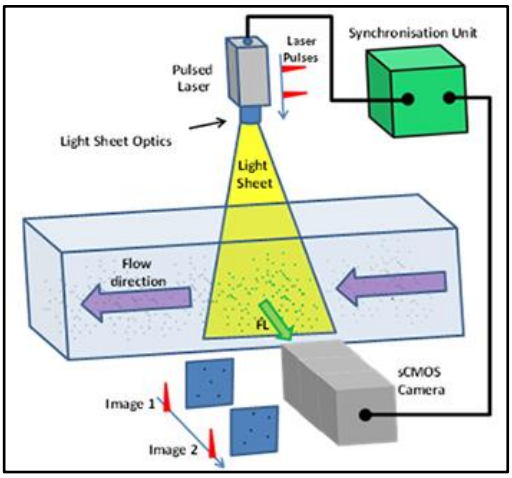

Figure 3: Sample of PIV system schematic with main components included [7]

The visualization of our system is powered by particle image velocimetry (PIV). Tiny reflective plastic polyamide particles are injected into the flow. A laser level is placed at the bottom of the tank. This laser shoots a laser plane into the flow and the light reflects off the particles. Note that the laser is class II, which means that it is safe for use as the intensity causes the eyes to naturally look away. A separate phone is used on the side of the device. A software on the phone follows the reflective particles to determine the velocity profile of the fluid and the particle velocities as shown in Figure 4 below.

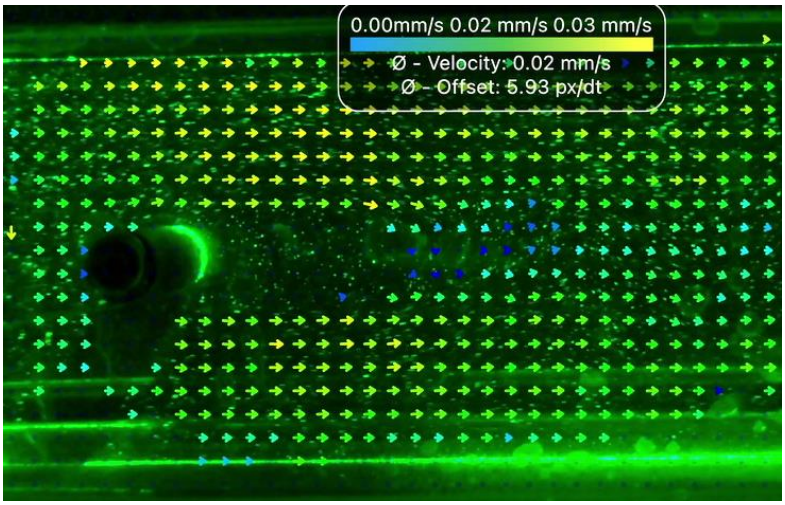

Figure 4: Sample of SmartPIV app from Cierpka et al. [8] with arrows describing velocity

The laser is on a track to allow it to be moved in the x-direction (along the 40" length of the tank) and the z-direction (along the 8" width of the tank). The movement in the x-direction will show the fluid being developed and eventually fully developed. Moving the laser in the z-direction will show the same fully developed velocity profile and magnitude, supporting the infinite plate conditions. One key consideration was understanding particle size in fluid flow. Introducing the particles needed for PIV makes the flow non-Newtonian, but given a small enough particle concentration and small enough particle size, the difference is negligible. In other words, the resolution of the tracking software is not detailed enough to see the difference in Newtonian and non-Newtonian flow. A preexisting app for PIV tracking was used for the project. SmartPIV is able to model the flow by identifying particles and interpolating velocities based on the phone camera's frame rate. The velocities map to particles with arrows color coded based on the range of velocities detected.

Design Process

Our design has been iterated as we have redefined constraints, reevaluated the relative importance of our objectives, and recalculated system behavior. The system was first defined in terms of the cart and the tank. The overall dimensions of both were determined by the need to construct an easily transportable system on a cart of standard size. Initially, the tank was 5" by 5" by 40". This fairly small tank meant a low volume of fluid was moving through the system, allowing a weaker and lower-cost pump to be used and less material for the tank's construction. Static analysis and fluid mechanics calculations were performed to verify the system's robustness under mechanical loading as well as to ensure that the fluid was reaching a desired laminar velocity; however, this size was challenged during the Capstone analysis presentation. The 5" by 5" cross section was a poor choice since the equal aspect ratio would make it difficult to approximate flow between two flat plates. While we originally stuck by the 5" by 5" cross section in order to maximize the height of the tank (allowing students to more easily see the relevant velocity profile), we reevaluated the relative importance of maintaining a 5" height. Understandably, the need to approximate flow between two flat plates prevailed, with the new tank dimensions set to 3" by 8" by 40". Static and flow analysis were recalculated to validate the outputs altered by the new dimensions. FEA and CFD calculations supported the numerical results.

The dimensions of the tank were also influenced by the constraints of PIV accuracy. The PIV software was found to be accurate to one pixel [8]. This accuracy depends on the phone camera's resolution and the scale of the viewing window to the phone screen. The challenge here was to identify the best viewing window that captures the full effects of shear on the velocity profile and is within the camera's focus range. An iPhone with a 1080 px camera resolution and a 3" x 3" viewing window results in a measurement accuracy of ±0.003" in/s.

The ideal velocity of the tank is highly dependent on phone camera resolution and the capabilities of SmartPIV. The SmartPIV software can detect 20 micron particles moving at an average velocity of 0.18m/s [8]. This means that the desired 3" x 3" window space with a 1080 x 1080 px resolution would be best at tracking particles moving at an average velocity of around 0.72 in/s. Flow analysis indicates a 3" tank height results in a theoretical maximum particle velocity of 0.94 in/s and a theoretical average particle velocity of 0.47 in/s, which is close to our desired particle velocity of 0.72 in/s.

In addition to the alterations to the tank dimensions, the design of the tank supports bracing the bottom of the tank has also changed throughout the process. In the initial design, 80/20 extrusion supported the bottom of the tank. In order to secure the position of these extrusions, the walls of the acrylic tank would be lengthened to sandwich the extrusions. Holes drilled in this acrylic overhang would allow the acrylic to be bolted to the 80/20 extrusions; however, the additional holes would add additional undesirable stress to the tank. This design was challenged by Professor Hashemi, who provided suggestions to simplify the assembly. The original design overconstrained our model. In other words, the tank will not move in the y and z-directions, only the x-direction. Support plates would be sufficient to constrain the movement of the tank. FEA calculations verified that the support plates could handle the weight. This simplified design mitigated risk while providing stability, lowering weight, and reducing cost.

The mechanism that enables the rotation of the tank also underwent iteration. The initial design consisted of a large arcing plate mounted at the bottom of the tank. The plate had holes along its length where a pin could be fastened in different locations, changing the angle of the tank's tilt. While the design was simple and allowed the user to choose a range of angles, users could struggle to lift the tank and swap the pin's location at the same time. In addition, our client informed us that they only needed the tank to switch between two positions: one with no tilt at all, and one with a noticeable angle. As a result, the plate was

swapped out in favor of gas struts and "trunk" hinges. The gas strut applies force to help the user lift the tank with ease, and the truck hinges lock the system at our desired 30 degree angle.

The system that circulates fluid through the tank also increased in complexity as our understanding of our model grew. Our fluid system initially consisted of a pump, fluid piping, and the main tank. The system was designed as a closed loop system with a reservoir to supply fluid. To implement these controls, pressure transducers, check valves, relief valves, and manual ball valves were added. These values would allow the user the ability to control and manage system flow, while the pressure transducers would allow the user to monitor the relevant pressure gradient. A flow straightener was also added to break up the jet of fluid entering the tank as shown in the Appendix. During the engineering analysis presentation, Professor Allshouse raised a question about filling the tank, specifically on how we planned on eliminating bubbles within the flow. This was a critical question when the tank had to be emptied and refilled regularly in order to maintain cleanliness. To tackle this problem, the reservoir was removed, lids were added to the top of the tank, and a release valve was implemented in order to enable the user to fill the tank while limiting bubbles.

Results

The constructed system consists of a tank where fluid and particles are circulated via a pump. The pressure difference created by the pump is quantified by the two pressure transducers mounted to the top of the tank. SmartPIV is used to report the velocity of a plane of polyamide particles illuminated by a laser. The four assumptions used to simplify the Navier-Stokes equations can be verified by the PIV system:

- The steady state assumption is verified when the velocity of particles at each coordinate is constant.
- The infinite plates assumption is verified in the y-plane (along the 3" height of the tank) when the particle velocities are oriented primarily in the direction of flow.
- The plane flow assumption is verified when the velocity profiles are constant as the plane of illuminated particles move along the z-plane (along the 8" width of the tank).
- The fully developed condition is verified when the velocity profiles are constant as the phone camera moves along the x-plane (along the 40" width of the tank) within the fully developed region.

We set the groundwork for a potential phase two project. Our current system visualizes Poiseuille pressure-driven flow. Our pump provides a pressure gradient that drives our fluid flow. Another scenario often seen in Navier-Stokes problems is Couette shear-driven flow, where a moving plate drives the flow. Early in the design process, we considered implementing a conveyor belt, but the tank dimensions required for Couette flow interfered with the dimensions required for Poiseuille flow. A phase two project visualizing shear-driven flow would approximate a wider variety of Navier-Stokes situations, enabling enhanced learning opportunities for students. In addition, user interaction could be improved for our system. For instance, manual screws are used to adjust the PIV system location in our current design. A way to improve this mechanism would be to use a plunger pin to secure the aluminum bars when sliding. This would reduce the time and energy required from the user when adjusting the PIV laser location.

In addition to our system, we created materials for students to learn the assumptions surrounding the Navier-Stokes equations. These materials supplement the classroom learning experience and give students a guided route to learning with our rig. It may take a full semester to receive numerical results from grades and a few more semesters for statistical certainty; however, we can gauge rough conceptual understanding by presenting a short lesson to students and asking for their impressions.

Summary and Impact

Navier-Stokes are a set of fluid equations that describe the motion of viscous fluids. These equations are also a millennium problem [9], a famous classical problem without a solution. These equations do not have a mathematical proof to show that solutions exist and that they are unique. Navier-Stokes may hold the keys to truly understanding the motion of a morning breeze and roaring waves of the ocean. The first step in learning how to solve these equations is utilizing certain scenarios that simplify the equations into a solvable form. Our design will mimic these scenarios to help students understand the assumptions and why they are valid. A physical model allows them to actively see the assumptions come into play in real life and in real time. Designing this project strengthened our team's grasp of Navier-Stokes. The next step is bringing it into the classroom to see how it helps students and what improvements can be made. In the greatest likelihood, it will help students perform better in class and achieve higher grades. It will help them in future courses with fluid dependence like heat transfer. Engineers rely on basic initial estimations to move forward with designs. If students can draw on assumptions made in Navier-Stokes, they can better predict solutions to practical fluids problems. There is a small chance that this rig can become a stepping stone in helping a great mind solve the Navier-Stokes equations, ushering in a new wave of math, science, and technology.

References

[1] F. M. White, *Fluid Mechanics*, 8th ed. New York, NY: McGraw-Hill, 2016.

[2] D. L. Newman, M. Stefkovich, C. Clasen, M. A. Franzen, and L. K. Wright, "Physical models can provide superior learning opportunities beyond the benefits of active engagements," *Biochemistry and Molecular Biology Education*, vol. 46, no. 5, pp. 435–444, 2018, doi: 10.1002/bmb.21159. [Online]. Available: https://onlinelibrary.wiley.com/doi/abs/10.1002/bmb.21159.

[3] Y. J. Dori and M. Barak, "Virtual and Physical Molecular Modeling: Fostering Model Perception and Spatial Understanding," *Journal of Educational Technology & Society*, vol. 4, no. 1, pp. 61–74, 2001 [Online]. Available: https://www.jstor.org/stable/jeductechsoci.4.1.61.

[4] Fluids Explained. "Laminar Flow, Turbulent Flow and Reynolds Number (Lesson 3, Part 2)" *Youtube video*, 2:29. February 5, 2021. https://www.youtube.com/watch?v=vhDaCZZ0Sc4

[5] J. X. Chen and N. da Lobo, "Toward interactive-rate simulation of fluids with moving obstacles using Navier-stokes equations," *Graphical Models and Image Processing*, vol. 57, no. 2, pp. 107–116, 1995. doi:10.1006/gmip.1995.1012

[6] T. Persoons, "Measuring flow velocity and turbulence fields in thermal sciences using particle image velocimetry: A best practice guide," *Advances in Heat Transfer*, pp. 37–87, 2022. doi:10.1016/bs.aiht.2022.07.001

[7] Andor, "Guide to PIV Mode for iStar sCMOS Camera- Oxford Instruments," *andor.oxinst*. https://andor.oxinst.com/learning/view/article/piv-mode-for-istar-scmos.

[8] C. Cierpka, H. Otto, C. Poll, J. Hüther, S. Jeschke, and P. Mäder, "SmartPIV: flow velocity estimates by smartphones for education and field studies," *Exp Fluids*, vol. 62, no. 8, p. 172, Jul. 2021 [Online], doi: 10.1007/s00348-021-03262-z.

[9] J. A. Carlson, A. Jaffe, and A. Wiles, *The Millennium Prize Problems*. Providence, RI: American Mathematical Society, 2006.

Appendix: Engineering Analysis

In order to visualize flow between two flat plates, the flow within our system must approximate the expected theoretical behavior. The system needs to quickly attain fully developed laminar flow. In the fully-developed laminar flow region, the velocity profile's shape should remain roughly constant. To achieve this, a honeycomb flow straightener placed in the tank near the entrance diffuses the jet created by the inlet pipe. Without the straightener, the flow's velocity profile would more closely resemble a jet instead of the desired laminar velocity profile. To ensure the jet effects are fully mitigated, the geometry of the flow straighteners were adjusted based on CFD simulations. As a result, the current flow straighteners' design consists of a honeycomb mesh with a finer mesh near the entrance pipe.

The analysis was conducted in the three steps. A simplified model of the fluid within the tank was constructed in SOLIDWORKS. The model was imported into ANSYS Fluent R2 where it was meshed using the watertight geometry workflow. Mass flow input and output boundary conditions were assigned to the inlet and outlet pipes respectively. After running the simulation, the resulting velocity information was processed in MATLAB. The geometry of the flow straighteners were adjusted based on results and the system was re-analyzed for each iteration.

Four iterations of the flow straighteners influenced the final design as shown in Figure 5 below. The honeycomb of iteration "A" (Figure 5a) consisted of hexagons with an inscribed diameter of 0.500 in (12.69 mm), a wall thickness of 0.013 in (0.33 mm), and a length of 1.575 in (40 mm). Iteration "B", (Figure 5b) consisted of two flow straighteners with the same dimensions as "A", but each with a length of 0.787 in (20 mm). The second straightener's pattern was slightly offset compared to "A". Iteration "C" (Figure 5c) consisted of a single flow straightener where the hexagons directly in front of the inlet pipe were solid rather than hollow. Iteration "D" (Figure 5d) had the same pattern as "A" with a finer honeycomb mesh: each hexagon had an inscribed diameter of 0.256 in (6.5 mm).

(a) (b) (c) (d)

Figure 5: a) Iteration "A" of the flow straightener, b) Iteration "B" of the flow straightener consisted of two offset honeycomb patterns, c) Iteration "C" blocked flow directly in front of the inlet pipe, d) Iteration "D" consisted of a fine honeycomb mesh

As shown in Figure 6 on the next page, the final iteration combines the modifications of iterations "B", "C", and "D". It consists of two flow straighteners with hexagons with an inscribed diameter of 0.434 in (11.02 mm), a wall thickness of 0.079 in (2 mm), each with a length of 0.750 in (19.05 mm). The honeycombs directly in front of the inlet for both straighteners were particularly fine, with an inscribed diameter of 0.127 in (3.23 mm).

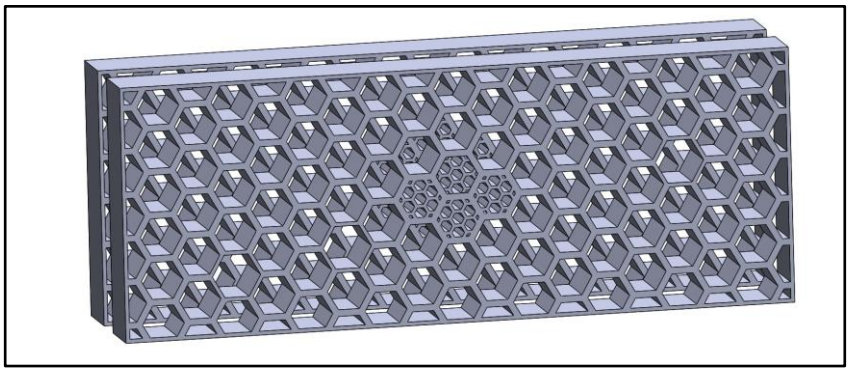

Figure 6: The final iteration of the flow straighteners consist of two straighteners with a particularly fine honeycomb mesh at the entrance pipe

For every iteration, a simplified CAD model was first constructed in SOLIDWORKS with the corresponding flow straightener. The solid bodies in the model represent the volume of fluid in the system. The faces of each solid body represent the boundaries where the walls of the tank, the pipes, or the flow straighteners prevent fluid flow. Additional solid bodies were used as bodies of influence, which helped refine the mesh in Fluent. The 3D double precision solver was selected to obtain the most accurate results. The model was meshed using the watertight geometry workflow. Important mesh settings and the resulting outputs are organized in Table 1 below.

Table 1: Flow Straightener Mesh Settings

	Iteration 1 (Original)	Iteration 2 (Double)	Iteration 3 (Obstacle)	Iteration 4 (Fine Honeycomb)	Iteration 5 (Final)
Local Sizing *Use a body of influence?*	No	No	No	No	Yes, 1 mm target size, 1.1 growth rate
Surface Mesh *Min / Max Size (mm)*	1.5 / 6	1.5 / 6	1.5 / 6	1.5 / 6	1 / 8
Surface Mesh *Growth Rate*	1.1	1.1	1.05	1.1	1.2
Boundary Conditions	Mass flow inlet at entrance pipe, mass flow outlet at exit pipe	Mass flow inlet at entrance pipe, mass flow outlet at exit pipe	Mass flow inlet at entrance pipe, mass flow outlet at exit pipe	Mass flow inlet at entrance pipe, mass flow outlet at exit pipe	Mass flow inlet at entrance pipe, mass flow outlet at exit pipe
Boundary Layers	Default	Default	Default	Default	Default
Volume Mesh *Fill With*	polyhexcore	polyhexcore	polyhexcore	polyhexcore	polyhexcore
Volume Mesh *Min / Max Cell Length (mm)*	1 / 3	1 / 3	1 / 3	1 / 3	1 / 8
Cell Count	941121	1240144	1285075	1264994	2445419
Average / Max Skew	0.05 / 0.89	0.06 / 0.93	0.06 / 1.96	0.07 / 0.79	0.03 / 0.50
Average / Min Orthogonal Quality	0.93 / 0.07	0.90 / 0.05	0.90 / 0.05	0.88 / 0.06	0.90 / 0.07

The resulting mesh was loaded into Fluent's solution setup with a pressure-based, steady state solver. The laminar model was chosen to best approximate the behavior of laminar flow within our system. The Reynolds-Averaged Navier-Stokes (RANS) turbulent models were avoided with the assumption that no significant turbulent effects were present in the model. The fluid density was set to 1193.4 kg/m^3 and the fluid viscosity was set to 0.035132 Pa*s based on the properties of a 70% glycerin-water mixture. The mass flow rates at the pipe inlet and outlet were set to 0.22 kg/s based on previous calculations relating the dimensions of our system and our chosen pump. All residuals (continuity, x-velocity, y-velocity, z-velocity) were set to 0.0001. In terms of the solution methods, Green-Gauss cell-based, standard pressure, and first order upwind were chosen to improve the speed of the solver. Hybrid initialization was used to improve accuracy.

After the solution converged, the results were exported as an ASCII file and analyzed using MATLAB. The velocity at tank cross sections perpendicular to the flow were graphed on a colormap. The roughly parabolic velocity profiles describing the development of the flow were also graphed for each iteration. The results of the analysis for the first and last iteration are shown in Figure 7 and 8 below.

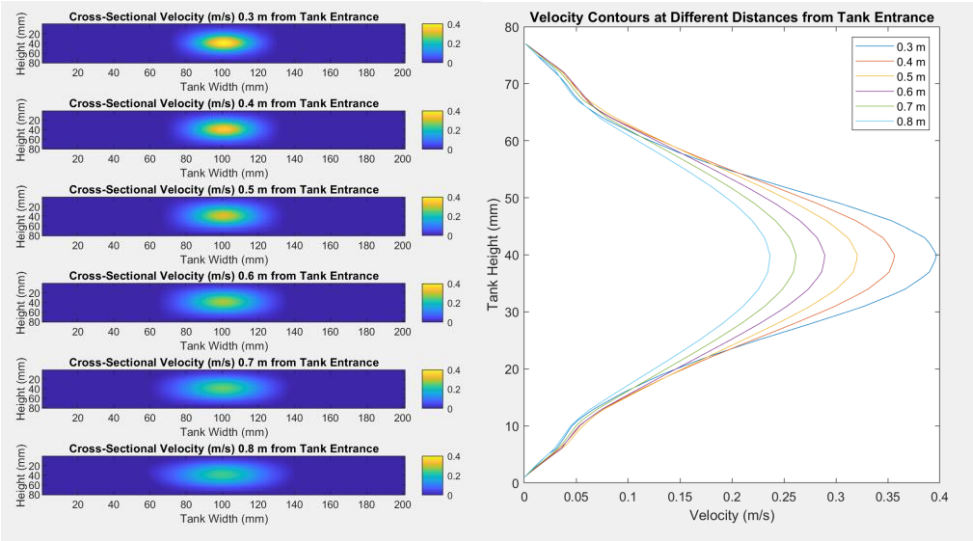

Figure 7: Tank velocity resulting for original flow straightener iteration

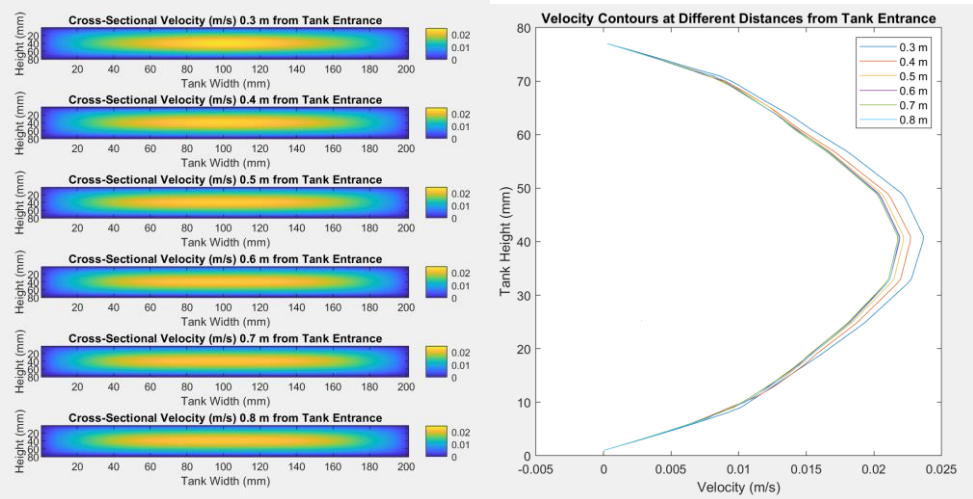

Figure 8: Tank velocity resulting for final flow straightener iteration

The results of the original honeycomb highlighted the weaknesses of our first iteration. The colormap above revealed that the high velocity regions remained in the center of the tank. The shape of the velocity contours reflected this jet-like behavior, with slow velocity regions near the walls and fast velocity regions near the center. This shape deviated from the target parabolic behavior.

For jet dispersion, two flow straighteners were used. The results of this test indicate that high velocity regions were better dispersed with maximum velocity decaying less, but still not at an ideal rate. A flow straightener with an obstacle right in front of the entrance pipe was designed as an alternative method for jet dispersion. The shape of the velocity contour was much closer to parabolic and thus much closer to ideal; however, the overall velocity dropped significantly to around 0.025 m/s (0.98 in/s). The maximum velocity also appeared to be changing more than was desired. As an additional alternative, a single flow straightener with small honeycombs was designed. The results were very similar to those with two flow straighteners, suggesting that the use of two offset flow straighteners was fairly equivalent to using a fine honeycomb mesh.

Based on the results of these first four iterations, the final iteration "E" aimed to combine the flow dispersion of iteration "C" while reducing decay more effectively than iterations "B" and "D". As a result, two flow straighteners were used to mitigate decay and small honeycombs were used instead of a solid obstacle in front of the inlet pipe. The resulting velocity contours are very close to parabolic and the maximum velocity changes little between 0.3 m to 0.8 m from the entrance. While there is a significant loss in velocity compared to the other iterations at 0.022 m/s (0.87 in/s), this slow velocity more closely matches the expected velocity from previous calculations.

While the CFD analysis suggests that the system will produce the desired fluid behavior, the computational model is a simplification of the physical system. The tank is modeled as a watertight, fully smooth rectangular prism, ignoring geometric oddities such as pipe fittings or pressure transducers that exist in the actual construction. These geometric oddities coupled with the difficulty of completely eliminating air bubbles could affect the flow in unexpected ways. The non-ideal behavior of the pump may also interfere with the desired flow. The boundary conditions assume a constant mass flow rate of 0.22 kg/s at the inlet and outlet. The pump is capable of achieving the ideal mass flow rate, though the actual mass flow rate will likely vary. In addition, the pump exhibits sinusoidal behavior, pumping in short waves rather than constantly, which may adversely affect the consistency of the laminar velocity profiles.

Non-ideal model setup may also affect the validity of the CFD results. According to Table 1, the maximum skew and minimum orthogonal quality tends to be respectively higher and lower than ideal. These indicators could be neglected because there were very few cells with high skew and low orthogonal quality, as signified by the low average skew and high average orthogonal quality. The solution setup was also using the first order upwind scheme, which tends to be less accurate than second order upwind. The analysis would ideally be rerun with second order upwind, but limited time meant first order upwind was a better choice considering the high cell counts.

This engineering analysis owes much to Professor Allshouse, whose assistance with CFD was instrumental. His review of several intermediate iterations helped identify critical errors in the CFD mesh setup. Moreover, his feedback produced the initial MATLAB post-processing code that formed the basis for later adjustments. In addition, Professor Matherne's review of the CFD results ensured each iteration of the flow straighteners was focused on moving towards the goal of developing parabolic velocity profiles.